Carbohydrate Polymers 86 (2011) 941–947

Contents lists available at ScienceDirect

Carbohydrate Polymers

journal homepage: www.elsevier.com/locate/carbpol

Isothermal crystallization kinetics of thermoplastic starch/poly(lactic acid) composites

Jie Cai[a,b], Miao Liu[a,b], Li Wang[a,b], Kunhua Yao[a,b], Sha Li[a,b], Hanguo Xiong[a,b,*]

[a] College of Food Science and Technology, Huazhong Agricultural University, Wuhan 430070, China
[b] Research Institute of comprehensive utilization of Biomaterials, Huazhong Agricultural University, Wuhan 430070, China

ARTICLE INFO

Article history:
Received 27 April 2011
Received in revised form 5 May 2011
Accepted 24 May 2011
Available online 1 June 2011

Keywords:
Thermoplastic starch
Poly(lactic acid)
Isothermal crystallization kinetics
DSC

ABSTRACT

The thermoplastic starch/poly(lactic acid) (TPS/PLA) composites were prepared using PLA melt blending with glycerol plasticized-starch. A systematic study of the isothermal crystallization kinetics of TPS/PLA composites was performed by differential scanning calorimetry (DSC) at different crystallization temperatures (T_c). The analysis based on the Avrami theory, which was applied to describe the process of isothermal crystallization, indicated that the spherulite growth rate, overall crystallization rate, and activation energy (ΔE_a) of TPS/PLA composites were remarkably affected by the incorporation of TPS. TPS acts as a nucleating agent, improving the crystallinity of PLA in the composites. Furthermore, according to Lauritzen–Hoffman kinetic theory, the fold surface free energy (σ_e) of PLA blends is found to be higher than that of neat PLA, leading to a higher work of chain folding (q) and is ascribed to a general constraint of the PLA chain mobility in the composite melt due to the presence of TPS.

1. Introduction

With economic and social development, the consumption of non-renewable, petroleum-based chemicals for the synthesis and manufacture of commodity polymers in various applications has generated considerable environmental problems (Kumar, Mohanty, Nayak, & Parvaiz, 2010). In recent years, much attention has been focused on the development of biodegradable and biocompatible polymers with a primary aim to address these problems in the polymer industry. In this direction, poly(lactic acid) (PLA) is one of the most promising candidates for environment-friendly composite development (Velde & Kiekens, 2002). Unlike petroleum-based plastics, biodegradable green plastic PLA is produced from lactic acid, which can be obtained from 100% renewable agricultural resources such as corn or sugar beets. Besides, PLA can be fabricated readily, has good mechanical properties, and thermal plasticity, thus being a promising polymer for various applications such as drug delivery, tissue engineering, food packing and bottle containers. However, the inherent brittleness characteristics and low glass transition temperature (around 333 K) of PLA are its major defect limitations, preventing its widespread industrial use (Bastioli, 2001; Kumar et al., 2010; Petersen, Nielsen, & Olsen, 2001). Moreover, its relatively high cost lowers the possibility of commercialization.

Starch is one of the most abundant polymeric materials derived from renewable resources (Cao, Mohamed, Gordon, Willett, & Sessa, 2003). It is cheap, fully biodegradable (Elsenhaber & Schulz, 1993; Leloup, Colonna, & Ring, 1991), and has been widely used to make biodegradable materials, such as the composites of starch/PE (Wang & Yu, 2005), starch/LDPE (Huang, Roan, Kuo, & Lu, 2005; Nakamura, Cordi, Almeida, Duran, & Mei, 2005; Pedroso & Rosa, 2005), and starch/PCL (Chen et al., 2006; Rosa, Lopes, & Calil, 2005), among others.

To broaden application of PLA, studies on PLA blends with other low-cost biodegradable materials have been carried out. The preparation of starch/PLA composites has been considered a promising method for improving the thermal properties and lowering overall cost. Due to the poor adhesion of starch and PLA, however, previous reports have shown that starch/PLA composites have rather poor mechanical properties (Ke & Sun, 2000; Kim, Chin, Yoon, Kim, & Jung, 1998). To improve interfacial adhesion of PLA blends, glycerol (a reactive processing agent) has been added as a plasticizer to the starch in the current study. Starch prepared in this similar fashion is known as thermoplastic starch (TPS) (Rodriguez-Gonzalez, Ramsay, & Favis, 2004). The thermoplastic starch/poly(lactic acid) (TPS/PLA) composite materials, prepared by PLA melt blending with glycerol plasticized-starch, balances between the high performance of PLA and the inexpensive qualities of starch. This composite has the potential to economize petroleum resources, and to develope new nonfood uses for starch.

* Corresponding author at: College of Food Science and Technology, Huazhong Agricultural University, Wuhan, Hubei 430070, China. Tel.: +86 27 87288377, fax: +86 27 87286608.
E-mail address: xionghanguo@163.com (H. Xiong).

0144-8617/$ – see front matter © 2011 Elsevier Ltd. All rights reserved.
doi:10.1016/j.carbpol.2011.05.044

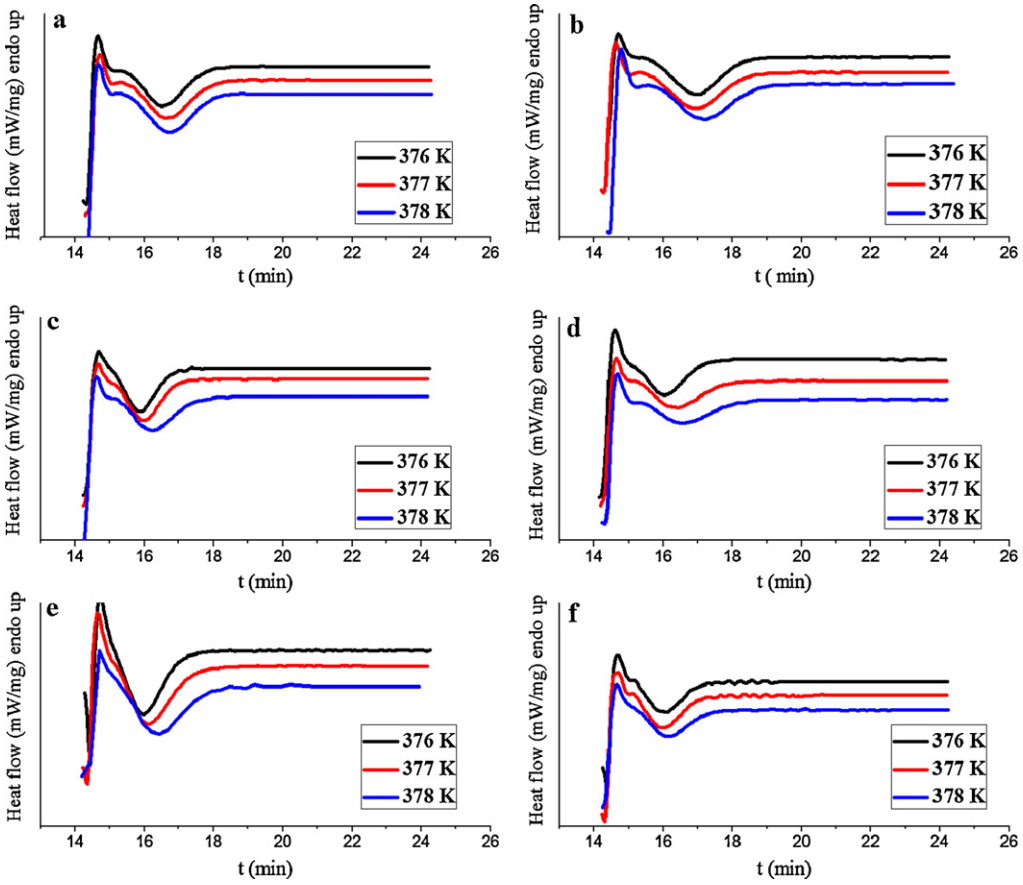

Fig. 1. The DSC traces of samples isothermally crystallized at the specified temperature: (a) TPS:PLA = 0:100; (b) TPS:PLA = 20:100; (c) TPS:PLA = 40:100; (d) TPS:PLA = 60:100; (e)TPS:PLA = 80:100; (f)TPS:PLA = 80:100 (by weight).

The analysis of the crystallization behavior of polymer, allowing for the design of materials with desirable properties, is important in the field of polymer physics. In particular, the filler in a polymer will affect substantially the crystallization behavior of polymer-based composites (Kundu & Biswas, 2003). Understanding crystallization kinetics contributes to the study on the crystallization behavior of polymers. This paper aims to analyze the behavior of polymer/filler composites using the TPS, we thoroughly investigated the isothermal crystallization kinetics of a TPS/PLA composite system. Crystallization kinetic parameters based on the isothermal crystallization of neat PLA and TPS/PLA composites were determined using differential scanning calorimetry (DSC) and calculated according to the Avrami method.

2. Experimental method

2.1. Materials

Poly(lactic acid) (PLA) pellets used in this investigation were acquired from Shenzhen Guanghua Industrial Co., Ltd with a molecular weight $M_n = 1.4 \times 10^4$ g/mol. Granular (native) corn starch was supplied by Tianjin Tingfung Starch Development Co., Ltd. Glycerol was produced by China National Pharmaceutical Group, with a boiling point of 563 K (101.3 KPa).

2.2. Preparation of TPS/PLA composites

During preparation, PLA was dried at 353 K for 5 h and corn starch was dried at 373 K for 4 h in a forced air oven, respectively. Besides, corn starch was modified by glycerol as a plasticizer (glycerol/starch 30/100 by weigh) to obtain thermoplastic starch (TPS). After that, the poly(lactic acid) and thermoplastic starch were mixed in a roller at 448–453 K for 10–15 min. The resulting sheet was compressing molded at 448 K into 1–1.5 mm thick sheet under a pressure of 9 MPa for 10 min, and kept at in room temperature. TPS/PLA blends were prepared by mixing the stock solutions to achieve the following weight ratios of TPS to PLA: (a) 0/100; (b) 20/100; (c) 40/100; (d) 60/100; (e) 80/100; (f) 100/100, respectively.

2.3. Differential scanning calorimetry (DSC) analysis

A Nexus DSC 204F1 was used to record isothermal cold crystallization behavior of the samples. Standard indium was employed for the temperature and heat flow calibration at each cooling rate in the measurement. Samples of 5–10 mg were weighed accurately and encapsulated in aluminium pans. Additional an empty aluminium pan was placed in reference compartment as means of improving the thermal response. All the thermograms are presented with downward deflection in DSC scans.

The samples were heated from 293 K at the rate of 30 K/min to 473 K above the melting temperature and then kept at this temperature for 5 min to erase previous thermal history of melt characterization. Subsequently samples were rapidly cooled to the desingated crystallization temperature (T_c) of interest 376, 377 and 378 K at the rate of 30 K/min to obtain the crystallization curve as a function of temperature. The sample was held at desired isothermal temperature for 10 min unitl the crystallization process was no change in the heat flow. After which, the samples were heated to 473 K at a rate of 10 K/min to obtian melting temperature (T_m).

During the analysis, dry nitrogen gas was purged into the DSC cell with a flow rate of 60 mL/min to prevent thermal degradation. There has been no change in sample weights after the completion of the all thermal analysis process.

3. Results and discussion

3.1. Isothermal crystallization behavior of the PLA and TPS/PLA composites

The isothermal crystallization thermograms of PLA and TPS/PLA composites obtained by cooling a molten polymer to the designated crystallization temperature (T_c) are shown in Fig. 1. In Fig. 1, as T_c increases, the crystallization exothermic peak roughly shifts to a higher value. The influence of T_c on crystallization in the TPS/PLA blends is stronger than in the neat PLA. Furthermore, the crystallization of pure PLA is strongly affected by TPS addition. The addition of TPS shortens the time to reach the crystallization half-time, indicating a faster crystallization rate, as shown in Table 1. This result suggests that during the isothermal crystallization, TPS acts as a nucleating agent and contributs to an improvement in the crystallinity of PLA blends.

The isothermal crystallization kinetics can be better visualized by evaluating the relative degree of crystalline conversion as a function of time at a constant temperature (Liu et al., 2010). The relative crystallinity (X_t) versus a different crystallization time (t) is calculated according to the following equation:

$$X_t = \frac{Q_t}{Q_\infty} = \frac{\int_0^t (dH_c/dt)\,dt}{\int_0^{t_\infty} (dH_c/dt)\,dt} \quad (1)$$

where Q_t and Q_∞ are the heat generated at time t and infinity, respectively, and dH_c/dt is the rate of heat evolution. X_t is obtained from the area of the exothermic peak of the isothermal crystallization analysis using DSC, and is plotted in Fig. 2 with respect to t. From Fig. 2, the characteristic sigmoidal isotherms roughly shift to the right along the time axis with increasing T_c, which means that the crystallization rate decreases.

3.2. Analysis based on the avrami theory

Assuming that relative crystallinity (X_t) increases with the crystallization time (t), the Avrami theory, usually used to study on the crystallization kinetics of polymers (Huang, Gu, & Ozaki, 2006), can be employed to analyze the isothermal crystallization process of PLA and TPS/PLA composites as below:

$$1 - X_t = \exp(-Kt^n) \quad (2)$$

To deal conveniently with the operation, Eq. (2) is usually rewritten in a double logarithmic form as follows:

$$\ln[-\ln(1 - X_t)] = \ln K + \ln t \quad (3)$$

where X_t is the relative crystallinity of the polymers at different temperatures or times, and t is the period of crystallization process. K and n values denote the crystallization rate constant and the Avrami exponent, respectively. K is a growth rate constant that accounts for both the nucleation and the growth rate parameters, and n is a mechanism constant that depends on the form of nucleation and the growth dimension.

The plots of $\ln[-\ln(1 - X_t)]$ versus $\ln t$ for each cooling rate (according to Eq. (3)) are shown in Fig. 3. Accordingly, the Avrami exponent n and the crystallization rate K are obtained from the slope and intercept, respectively, and are listed in Table 1. The crystallization process generally has usually treated in two stages: the primary crystallization stage (linear portion) and the secondary crystallization stage (nonlinear portion). Here, it is understood that the primary crystallization is caused by the outward clear growth of lamellar stacks. This deviation due to the occurrence of the secondary crystallization, which is attributed to the perfection of the internal spherulite crystallization and the spherulite impingement in the later stage of the crystallization process (Ge, Ding, Shi, & Fu, 2009; Run, Song, Wang, Bai, & Jia, 2009). However, the Avrami equation is generally assumed to be applicable only to the primary crystallization stage. For the isothermal crystallization process, a linear portion is approximately 30–70% of the relative crystallinity (Liao, Yang, Yu, & Zhou, 2007). Hence, the current study focuses only focus on the linear portion of the $\ln[-\ln(1 - X_t)]$ versus $\ln t$ plots for the isothermal crystallization of PLA and TPS/PLA composites.

Crystallization half-time, $t_{1/2}$, is another important crystallization kinetics parameter, is defined as the time taken from the start of the relative crystallinity until 50% completion. The half-time of crystallization ($t_{1/2}$) is calculated according to the following equation:

$$t_{1/2} = \left(\frac{\ln 2}{K}\right)^{1/n} \quad (4)$$

Usually, $t_{1/2}$ is employed to characterize the crystallization rate directly. Moreover, the growth rate of crystallization (G) is defined as the reciprocal of $t_{1/2}$, as follows:

$$G = \frac{1}{t_{1/2}} \quad (5)$$

The longer the crystallization half-time, the slower the crystallization rate.The dependence of $t_{1/2}$ and G on T_c for six samples from the previous equations is shown in Table 1.

In the Avrami expression, n provides qualitative information on the nature of nucleation and the growth processes (Ge et al., 2009). An n value that is close to three is related to a three-dimensional crystal growth (spherical structure) that results from an instantaneous athermal nucleation process. On the other hand, an n value that is between two and three represents a non three-dimensional truncated spherical structures that results from instantaneous nucleation controlled by diffusion process. Non-integral of n values indicate a combination of thermal and athermal nucleation mechanisms (Kalkar, Deshpande & Kulkarni, 2009). As shown in Table 1, the Avrami exponents n obtained were very close to one another and are within the range 2.0–2.8 (the values of n are between 2 and 3). On the other hand, the n values reported in the literatures are dispersed, ranging from 2 to 5.4 (Liao et al., 2007). The values obtained in the study are acceptable because the difference in values can be attributed to several factors such as the mechanism of nucleation, the form of crystal growth, and the difference in the techniques used in determining the values. Additionally, it is implied that the crystals gradual growth of two-dimensional morphology to a spherical three-dimensional morphology with a combination of thermal and athermal nucleation in the TPS/PLA systems.

The K values, which are related to nucleation rate and growth processes, are extremely sensitive to T_c. K decreases with increasing T_c in all TPS/PLA composites (Table 1), indicating that the crystallization rate is decreasing. Besides, the introduction of TPS significantly increases K, suggesting that TPS acts as an effective nucleating agent that accelerates the crystallization rate of PLA by providing nucleating sites and by reducing the melt viscosity of PLA.

As shown in Table 1, in most of the samples, the $t_{1/2}$ values increase with increasing T_c, which means slower crystallization rate. The $t_{1/2}$ values of the composites are lower than those of neat PLA, impling that TPS accelerates the crystallization of PLA in the composites, in accordance with the previous results. The results in Table 1 also agree with those inferred from Fig. 2.

Table 1
Avrami kinetic parameters and activation energy (ΔE) of neat PLA and TPS/PLA composites as function of crystallization temperature.

Samples	T_c (K)	$t_{1/2}$ (min)	G (min^{-1})	n	K (min^{-1})	ΔE (kJ/mol)
	376	2.02821	0.49305	2.5	0.12	
TPS/PLA (0/100 w/w)	377	2.03887	0.49047	2.3	0.14	−14.9
	378	2.01344	0.49666	2.1	0.16	
TPS/PLA (20/100 w/w)	376	1.67988	0.59528	2.3	0.22	
	377	1.77286	0.56406	2.4	0.18	−27.2
	378	1.77145	0.56451	2.4	0.18	
	376	1.72866	0.57848	2.8	0.44	
TPS/PLA (40/100 w/w)	337	1.25706	0.79550	2.8	0.37	−160.8
	378	1.52412	0.65612	2.5	0.25	
	376	1.31320	0.76150	2.2	0.38	
TPS/PLA (60/100 w/w)	377	1.58680	0.63020	2.3	0.24	−172.9
	378	1.73318	0.57696	2.0	0.23	
	376	1.24672	0.80210	2.3	0.42	
TPS/PLA (80/100 w/w)	377	1.39584	0.71641	2.3	0.32	−124.3
	378	1.55192	0.64436	2.4	0.24	
	376	1.24712	0.80185	2.4	0.41	
TPS/PLA (100/100 w/w)	377	1.20422	0.83041	2.5	0.44	−64.8
	378	1.38774	0.72060	2.4	0.32	

3.3. Activation energy of isothermal crystallization

The isothermal crystallization process of the neat PLA and TPS/PLA composites is assumed to be thermally activated. The activation energy of isothermal crystallization can be approximately described by the following form of the Arrhenius equation (Tjong, Chen, & Li, 1997):

$$K^{1/n} = K_0 \ \exp\left(\frac{-\Delta E_a}{RT_c}\right) \tag{6}$$

Eq. (6) can be rewritten in a logarithmic form as:

$$\left(\frac{1}{n}\right) \ln K = \ln(K_0) - \frac{\Delta E_a}{RT_c} \tag{7}$$

where K_0 and K values denote the pre-exponential factor and crystallization rate constant, respectively, R is the universal gas constant, and ΔE_a is the total crystallization activation energy. $\Delta E_a = \Delta F + \Delta\varphi$, where ΔF is the transformation activation energy or the activation energy of a unit crystallite crossing through the liquid–solid interface of a polymer, and $\Delta\varphi$ is the nucleation acti-

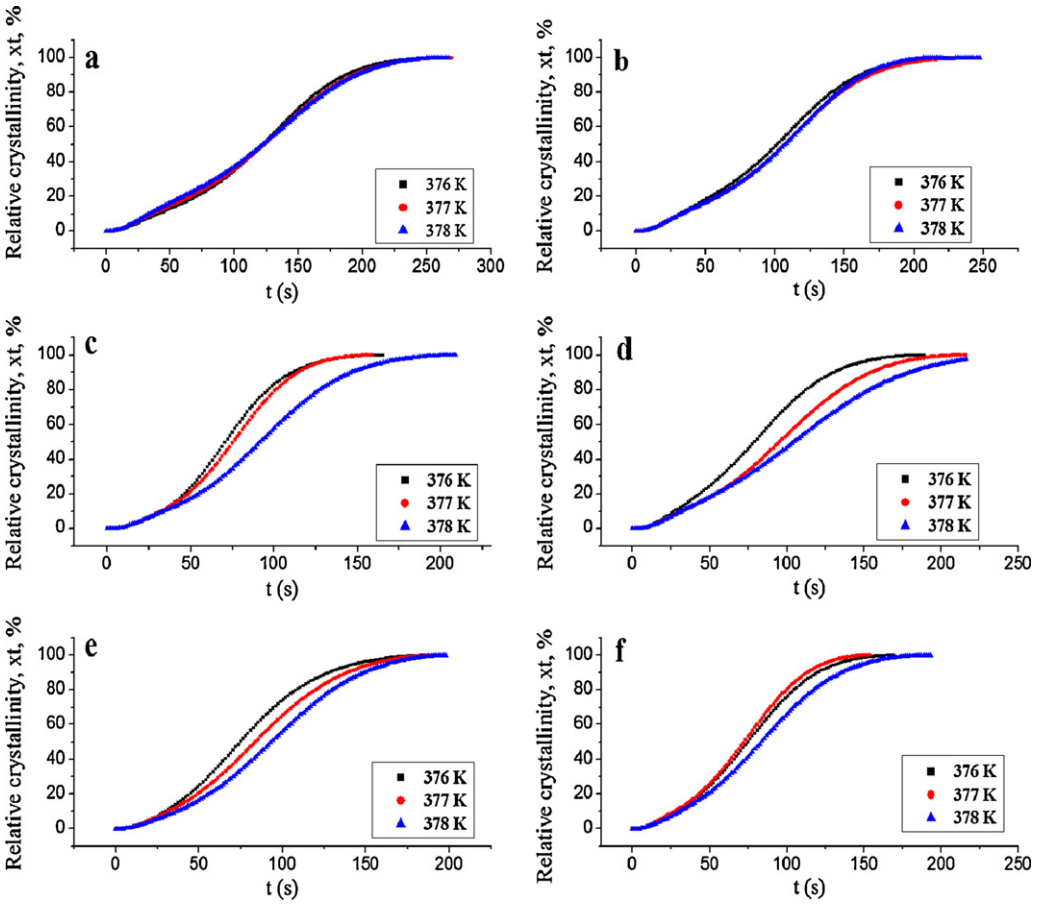

Fig. 2. Plots of X_t versus t for the isothermal crystallization of samples at the specified temperature: (a) TPS:PLA = 0:100; (b) TPS:PLA = 20:100; (c) TPS:PLA = 40:100; (d) TPS:PLA = 60:100; (e) TPS:PLA = 80:100; (f) TPS:PLA = 80:100 (by weight).

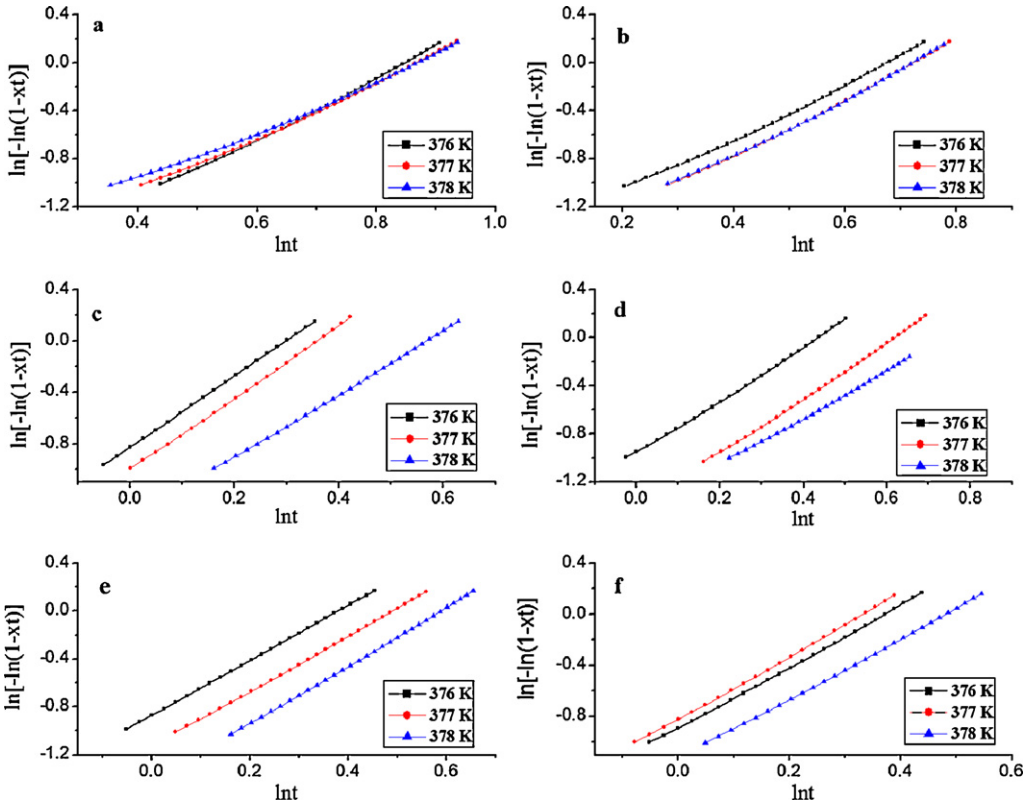

Fig. 3. Plots of $\ln[-\ln(1-Xt)]$ versus $\ln t$ for the isothermal crystallization of samples at the specified temperature: (a) TPS:PLA = 0:100; (b) TPS:PLA = 20:100; (c) TPS:PLA = 40:100; (d) TPS:PLA = 60:100; (e) TPS:PLA = 80:100; (f) TPS:PLA = 80:100 (by weight).

vation energy or the activation energy for the formation of a critical-sized nuclei at T_c. At a high T_c from the melt, the nucleation activation energy $\Delta\varphi/(RT_c)$ dominates at very low supercool degree, and the item of $\Delta F/(RT_c)$ in the multinomial expression is omitted. Thus, $\Delta\varphi$ approximately expressed the total activation energy ΔE_a (Ge et al., 2009). The crystallization activation energy (ΔE_a) is determined by the slopes of the plots of $(1/n)\ln K$ versus $1/T_c$ by Arrhenius equation (7).

In the current study, the ΔE_a values for neat PLA and TPS/PLA composites in primary crystallization are listed in Table 1. As is indicated in the table, the ΔE_a values are negative because the system releases energy when the polymer melt transforms into crystalline state. Additionally, ΔE_a is dependent on the TPS content of the composites and the TPS/PLA composites have lower ΔE_a values compared with those of neat PLA. This indicates that the addition of TPS into the PLA matrix can induce the heterogeneous nucleation and increase the crystallization ability of PLA during the crystallization processes. However, too much TPS colliding and intercrossing each other will hinder the movement and rearrangement of the PLA chain. Therefore, the value of ΔE_a increases when the TPS content exceeds the 60/100 (w/w) ratio in TPS/PLA composites.

3.4. Equilibrium melting point (T_m°)

To proceed with the quantitative analysis of crystallization behavior, especially the examination of the temperature dependence of the crystallization rate, the accurate determination of the equilibrium melting point possible is necessary (Zou, Tang, Fu, & Xiong, 2009). The reliable estimation of the equilibrium melting point can be made by careful DSC studies. Theoretically, the equilibrium melting point may be deduced by plotting the observed apparent melting temperature (T_m) against the crystallization temperature (T_c) (Hoffman & Weeks, 1962). The equilibrium melting point temperature can be extrapolated from the intersection of the resulting straight line to the line $T_m = T_c$ and the dependence of T_m on T_c is given by

$$T_m = T_m^\circ\left(1 - \frac{1}{2\beta}\right) + \frac{1}{2\beta}T_c \tag{8}$$

where T_m° is the equilibrium melting point and β describes the growth of lamellar thickness during crystallization. Under equilibrium conditions, β equals 1 (Kalkar et al., 2009). The values of T_m° listed in Table 2 are lower than the values reported in other studies. In addition, the values reported also differ from each other. The differences in the values can be attributed to the different PLA compositions and to the different treatment methods and detection techniques used in the studies (Liao et al., 2007).

3.5. Lauritzen–Hoffman (L–H) kinetic theory model

The thermodynamic parameters concerning the crystallization process can be determined from the calorimetric kinetic data obtained under isothermal conditions. The Lauritzen–Hoffman kinetic theory of polymer crystallization (Hoffman & Miller, 1997) is used to analyze the temperature dependence of the spherulitic growth rate G of neat PLA and blends by the following biexponential relationship:

$$G = G_0 \exp\left[\frac{U*}{R(T_c - T_\infty)}\right] \exp\left[\frac{Kg}{T_c \Delta Tf}\right] \tag{9}$$

Rearranging Eq. (9) as follows is most convenient:

$$\ln G + \frac{U*}{R(T_c - T_\infty)} = \frac{\ln G_0 - K_g}{T_c \Delta Tf} \tag{10}$$

where K_g is the nucleation parameter that reflects the regime behavior, G_0 is a pre-exponential factor that includes all

Table 2
Values of T_m°, K_g, σ_e and q for neat PLA and TPS/PLA composites.

Samples	T_m° (K)	$K_g \times 10^5$ (K^2)	$\sigma_e \times 10^{-2}$ (J/m^2)	q (kJ/mol)
TPS/PLA (0/100 w/w)	430.2	1.70	3.90	14.0
TPS/PLA (20/100 w/w)	431.6	3.07	6.82	25.3
TPS/PLA (40/100 w/w)	432.2	2.93	6.52	24.2
TPS/PLA (60/100 w/w)	432.8	3.88	8.63	32.0
TPS/PLA (80/100 w/w)	433.3	3.54	7.87	29.2
TPS/PLA (100/100 w/w)	433.5	2.77	6.52	22.8

temperature-independent terms, and R is the universal gas constant. U^* is the diffusional activation energy for the transport of segments to the crystallizable site at the liquid–solid interface taken as 6280 J/mol. ΔT is supercooling, defined as $T_m^\circ - T_c$, where T_c and T_m° denote the crystallization temperature and the equilibrium melt temperature, respectively. T_∞ is the hypothetical temperature where all motion associated with viscous flow ceases, which is usually assumed to be equal to $(T_g - 30)$K, and the term $f = 2T_c/(T_m^\circ + T_c)$ is the correction factor that accounts for the changes in heat of fusion as the temperature. In the Lauritzen–Hoffman equation, the crystallization growth rate G can be considered in Eq. (5) from a theoretical approach.

According to Eq. (10), the Lauritzen–Hoffman plots of $\ln G + U^*/[R(T_c - T_\infty)]$ versus $1/(T_c \Delta T_f)$ should yield a straight line with an intercept $\ln G_0$ and a slope $-K_g$. The nucleation constant K_g is listed in Table 2. As shown in Table 2, the K_g for the TPS/PLA composites is higher than those for neat PLA.

The factor K_g, a nucleation constant that contains contributions from the surface free energies of the lamellar crystals, is defined as:

$$K_g = \frac{r b_0 \sigma \sigma_e T_m^\circ}{k \Delta H_m^\circ} \tag{11}$$

where b_0 is the layer thickness of a single molecular layer (stem) in the crystal, which is 5.17×10^{-10} m. σ and σ_e are the lateral (side surface) and fold surface free energies of the growing crystal, respectively. ΔH_m° is the heat of fusion per unit volume, with a recommended value of $\Delta H_m^\circ = 1.11 \times 10^8$ J/m^2 and k is the Boltzmann constant. The value of r depending on the crystallization regime is a variable and theoretically assumes the value of 4 for the regimes I and III, and the value of 2 for the regime II, respectively.

To determine the regime in which the crystal growth occurs (in either I or II), the Lauritzen approximated Z-test equation is defined as:

$$Z \approx 10^3 \left(\frac{L}{2b_0}\right)^2 \exp\left[\frac{-X}{T_c \Delta T}\right] \tag{12}$$

where L is the crystalline substrate length. In Eq. (12), for regime I, $X = K_g$ and $Z < 0.1$, whereas, for regime II, $X = 2K_g$ and $Z > 1$. The possible L values in regime I and II for pure PLA and TPS/PLA composites were calculated. In this case for regime I, L was determined to be very low values than that of regime II, ranging from 0.1 to 43 nm, which are unreasonable substrate lengths compared with latter. Hence, crystallization in regime I was ruled out.

Once it is established that the crystallization occurs in regime II, the value of σ_e, the folding-surface energy, is calculated according to Eq. (11). The lateral surface free energy, σ, is often estimated by Thomas–Stavely empirical relation as follows (Lorenzo, 2001):

$$\sigma = \alpha(\Delta H_m^\circ)(a_0 b_0)^{1/2} \tag{13}$$

where a_0 and b_0 are the width and thickness of the stem added on the substrate whose values are 5.97×10^{-10} m and 5.17×10^{-10} m, respectively. The value of α for organic molecules is closer to 0.30, and $\alpha = 0.25$ has been chosen for estimation the surface free energy (σ) in the present case as appropriate to high melting polyesters (Hoffman, 1985). For PLA, σ is estimated as 1.54×10^{-2} J/m^2 using $\Delta H_m^\circ = 1.11 \times 10^8$ J/m^2 (the value of ΔH_m° suggested in the literature). According to Eq. (11), the σ_e values are illustrated in Table 2, which are close to the datas reported in other studies (Hoffman, Miller, Marand, & Roitman, 1992). Obviously, all the composites of TPS/PLA have a higher σ_e value compared with neat PLA. As σ_e is strongly correlated with the work of chain folding, which is well understood in terms of bending of polymer chain back upon itself, the higher σ_e value in composites suggests that there exist constraints on the mobility of the PLA chains in the interspherulitic regions due to the presence of TPS.

According to the Lauritzen–Hoffman theory, the work of chain folding per molecular fold (q) can be obtained from:

$$\sigma_e = \sigma_{e0} + \frac{q}{2a_0 b_0} \approx \sigma + \frac{q}{2a_0 b_0} \tag{14}$$

where q is the work of chain folding, is closely correlated with the molecular structure and the stiffness of the chain contributes to its magnitude, σ_{e0} is the value of σ_e when no work is required to bend the polymer chain back on itself, considering the conformational constraints on the fold imposed by the crystal structure. As a first approximation, σ_{e0} may be considered equal to the lateral surface interfacial energy σ. Thus, σ_{e0} is expected to be significantly less than $q/(2a_0 b_0)$ and may ultimately be set equal to zero (Kalkar et al., 2009). Therefore, Eq. (14) is usually rewritten in the following form:

$$q = 2a_0 b_0 \sigma_e \tag{15}$$

The values of q are summarized in Table 2. Compared with neat PLA, the increase in the value of q of TPS/PLA composites could be ascribed to a general constraint of the PLA chain mobility in the composite melt because of the addition of TPS.

4. Conclusions

A systematic study of the isothermal crystallization kinetics of the neat PLA and the TPS/PLA composites has been performed by differential scanning calorimetry (DSC) at designated crystallization temperature (T_c).

In this investigation, it can be concluded that the crystallization characteristics of PLA in TPS/PLA composites are affected by the introduction of TPS. The Avrami exponent n of the TPS/PLA composites is roughly larger than the crystallization process of neat PLA at the same T_c. Furthermore, the n values obtained in the study are very close, which are in the range of 2.0–2.8 (the values of n are between two and three). It is implied that gradual growth of two-dimensional morphology to a spherical three-dimensional morphology with a combination of thermal and athermal nucleation. The addition of TPS can significantly results in an increase in the crystallization kinetic constant K, suggesting that TPS can act as an effective nucleating agent and can accelerate the crystallization rate of PLA in the composites. After introducing a small amount of TPS, the crystallization half-time values ($t_{1/2}$) are all lower than those of neat PLA. Evidently, TPS can act as a nucleating agent for the PLA matrix, which is in accordance with the above results. The crystallization activation energy (ΔE_a) calculated from the Arrhenius formula and the composites of TPS/PLA have a lower value than those of neat PLA. Therefore, the addition of TPS component can

induce the heterogeneous nucleation and improve the crystallization ability of the PLA matrix during the crystallization processes. Compared with neat PLA, the fold surface free energy (σ_e) of PLA blends has a higher value, leading to a higher work of chain folding (q) and is ascribed to a general constraint of the PLA chain mobility in the composite melt because of the presence of TPS. It seems, therefore, that the changes of fold energies can be taken as evidence for the modification in structured folds of PLA in TPS/PLA composites.

Acknowledgment

The authors gratefully acknowledge the financial assistance supported by National Natural Science Foundation of China (No. 20976066).

References

Bastioli, C. (2001). Global status of the production of biobased packaging materials. *Starch*, *53*(8), 351–355.

Cao, X., Mohamed, A., Gordon, S. H., Willett, J. L., & Sessa, D. J. (2003). DSC study of biodegradable poly(lactic acid) and poly(hydroxy ester ether) blends. *Thermochimica Acta*, *406*(1), 115–127.

Chen, L., Qiu, X., Xie, Z., Hong, Z. K., Suna, J., Chen, X., et al. (2006). Poly(L-lactide)/starch blends compatibilized with poly(L-lactide)-g-starch copolymer. *Carbohydrate Polymers*, *65*(1), 75–80.

Elsenhaber, F., & Schulz, W. (1993). Moute carlo simulation of the hydration shell of double-helieal amylase: a left-handed antiparallel double helix fits best into liquid water the basis of two crystalline phase (I_a/I_β) system. *Journal of Applied Polymer Science*, *49*(8), 1491–1496.

Ge, C. H., Ding, P., Shi, L. Y., & Fu, J. F. (2009). Isothermal crystallization kinetics and melting behavior of poly(ethylene terephthalate)/barite nanocomposites. *Journal of Polymer Science Part B: Polymer Physics*, *47*(7), 665–668.

Hoffman, J. D. (1985). Theory of the substrate length in polymer crystallization: surface roughening as an inhibitor for substrate completion. *Polymer*, *26*, 1763–1778.

Hoffman, J. D., Miller, R. L., Marand, H. M., & Roitman, D. B. (1992). Relationship between the lateral surface free energy.sigma. and the chain structure of melt-crystallized polymers. *Macromolecules*, *25*(8), 2221–2229.

Hoffman, J. D., & Miller, R. L. (1997). Kinetic of crystallization from the melt and chain folding in polyethylene fractions revisited: theory and experiment. *Polymer*, *38*(13), 3151–3212.

Hoffman, J. D., & Weeks, J. J. (1962). Melting process and the equilibrium melting temperature of polychlorotrifluoroethylene. *Journal of Research of the National Bureau of Standards-A*, *66*, 13–18.

Huang, H., Gu, L. X., & Ozaki, Y. (2006). Non-isothermal crystallization and thermal transitions of a biodegradable, partially hydrolyzed poly(vinyl alcohol). *Polymer*, *47*(11), 3935–3945.

Huang, C. Y., Roan, M. L., Kuo, M. C., & Lu, W. L. (2005). Effect of compatibiliser on the biodegradation and mechanical properties of high-content starch/low-density polyethylene blends. *Polymer Degradation and Stability*, *90*(1), 95–105.

Kalkar, A. K., Deshpande, V. D., & Kulkarni, M. J. (2009). Isothermal crystallization kinetics of poly(phenylene sulfide)/TLCP composites. *Polymer Engineering and Science*, *49*(2), 397–417.

Ke, T., & Sun, X. (2000). Physical properties of poly(lactic acid) and starch composites with various blending ratios. *Cereal Chemistry*, *77*, 761–768.

Kim, S. H., Chin, I., Yoon, J., Kim, S. H., & Jung, J. (1998). Mechanical properties of biodegradable blends of poly(L-lactic acid) and starch. *Korea Polymer Journal*, *6*, 422–447.

Kumar, M., Mohanty, S., Nayak, S. K., & Parvaiz, M. R. (2010). Effect of glycidyl methacrylate (GMA) on the thermal, mechanical and morphological property of biodegradable PLA/PBAT blend and its nanocomposites. *Bioresource Technology*, *101*(21), 8406–8415.

Kundu, P. P., & Biswas, J. (2003). Influence of film preparation procedures on the crystallinity, morphology and mechanical properties of LLDPE films. *European Polymer Journal*, *39*, 1585–1593.

Leloup, V. M., Colonna, P., & Ring, S. (1991). Biotechnology and bioengineering. *Biopolymers*, *38*(2), 127–134.

Liao, R. G., Yang, B., Yu, W., & Zhou, C. X. (2007). Isothermal cold crystallization kinetics of polylactide/nucleating agents. *Journal of Applied Polymer Science*, *104*(1), 310–317.

Liu, H. X., Huang, Y. Y., Yuan, L., He, P. S., Cai, Z. H., Xu, Y. M., et al. (2010). Isothermal crystallization kinetics of modified bamboo cellulose/PCL composites. *Carbohydrate Polymers*, *79*(3), 513–519.

Lorenzo, D. L. M. (2001). Determination of spherulite growth rates of poly(L-lactic acid) using combined isothermal and non-isothermal procedures. *Polymer*, *42*(*23*), 9441–9446.

Nakamura, E. M., Cordi, L., Almeida, G. S. G., Duran, N., & Mei, L. H. I. (2005). Study and development of LDPE/starch partially biodegradable compounds. *Journal of Materials Processing Technology*, *162–163*, 236–241.

Pedroso, A. G., & Rosa, D. S. (2005). Mechanical, thermal and morphological characterization of recycled LDPE/corn starch blends. *Carbohydrate Polymers*, *59*(1), 1–9.

Petersen, K., Nielsen, P., & Olsen, M. (2001). Physical and mechanical properties of biobased materials-starch, polylactate and polyhydroxybutyrate. *Starch*, *53*(8), 356–361.

Rodriguez-Gonzalez, F. J., Ramsay, B. A., & Favis, B. D. (2004). Rheological and thermal properties of thermoplastic starch with high glycerol content. *Carbohydrate Polymers*, *58*(2), 139–147.

Rosa, D. S., Lopes, D. R., & Calil, M. R. (2005). Thermal properties and enzymatic degradation of blends of poly(ε-caprolactone) with starches. *Polymer Testing*, *24*(6), 756–761.

Run, M. T., Song, H. Z., Wang, S. J., Bai, L. B., & Jia, Y. H. (2009). Crystal morphology, melting behaviors and isothermal crystallization kinetics of SCF/PTT. *Composites Polymer Composites*, *30*(1), 87–94.

Tjong, S. C., Chen, S. X., & Li, R. K. Y. (1997). Crystallization kinetics of compatibilized blends of a liquid crystalline polymer with polypropylene. *Journal of Applied Polymer Science*, *64*(4), 707–715.

Velde, K. V., & Kiekens, P. (2002). Biopolymers: overview of several properties and consequences on their applications. *Material Properties*, *21*(4), 433–442.

Wang, S., & Yu, J. (2005). Compatible thermoplastic starch/polyethylene blends by one-step reactive extrusion. *Polymer International*, *54*, 279–285.

Zou, P., Tang, S. W., Fu, Z. Z., & Xiong, H. G. (2009). Isothermal and non-isothermal crystallization kinetics of modified rape straw flour/high-density polyethylene composites. *International Journal of Thermal Sciences*, *48*, 837–846.